Available online at www.eccomasproceedia.org
Eccomas Proceedia COMPDYN (2017) 3530-3542

ECCOMAS
Proceedia

COMPDYN 2017
6th ECCOMAS Thematic Conference on
Computational Methods in Structural Dynamics and Earthquake Engineering
M. Papadrakakis, M. Fragiadakis (eds.)
Rhodes Island, Greece, 15–17 June 2017

DYNAMIC ANALYSIS OF BRIDGE GIRDERS UNDER MOVING LOADS CONSIDERING WARPING AND MASS EFFECTS: NUMERICAL AND ANALYTICAL BEAM MODELS

João Serra[1], Ricardo Vieira[2], and Francisco Virtuoso[2]

[1] Instituto Superior Técnico
Lisbon
e-mail: joao.a.serra@tecnico.ulisboa.pt

[2] Instituto Superior Técnico
Lisbon
{ricardo.figueiredo.vieira,francisco.virtuoso}@tecnico.ulisboa.pt

Keywords: Vibrations, Dynamic Analysis, Thin-Walled Beams, Torsion, Warping, Bridges, High-Speed Railways, Moving Masses.

Abstract. *In order to perform efficient dynamic analyses of continuous high-speed railway bridges, a numerical and an analytical beam models are proposed in the present work. The behaviour of the bridge girder is described by a three-dimensional Euler-Bernoulli beam element, where an additional degree-of-freedom is considered at each beam-end, representing the cross-sectional warping. The structural response is determined by considering a modal analysis along with a direct integration scheme. The natural frequencies and vibration mode shapes are determined by the developed models. The trains are modeled as series of moving masses acting eccentrically at constant speed, allowing the corresponding inertial effects to be considered besides the gravitational force of mass.*

Peer-review under responsibility of the organizing committee of COMPDYN 2017.
doi: 10.7712/120117.5663.17518

1 INTRODUCTION

In the design of high-speed railway bridges, special consideration must be given to the torsional response of thin-walled girders. Therefore, warping of the cross-sections cannot be neglected in the structural dynamic analysis.

Performing dynamic analyses of bridges using shell finite element models allows to obtain accurate results, as long as detailed geometrical and material descriptions of the structures are known. However, using such models in early design stages is time consuming, which renders the evaluation of several structural solutions cumbersome. The use of beam models can minimize the time needed to calculate structural responses and prove good agreement with shell models. In the present work, a numerical and an analytical beam models are prosed.

The coupled governing equations of thin-walled beams were derived by applying the Hamilton's principle along with the Vlasov's beam theory.

In the developed numerical model, the behaviour of the bridge girder is described by a three-dimensional Euler-Bernoulli beam finite element, where an additional degree-of-freedom is considered to represent the cross-sectional warping. Lisi, [1], recently developed a beam finite element model for the static and the dynamic analysis of thin-walled beams under the action of a single eccentric moving force. The present work extends Lisi's study towards the inclusion of arrays of moving masses. Other relevant studies on coupled lateral bending-torsional vibrations of beams under moving loads are those of Michaltsos et al., [2][3][4].

The proposed analytical model allows to obtain the structural response of continuous beams with bending-torsional coupling in an exact sense. The formulation presented is based on the work done by Chan and Ashebo, [5], where the problem of uncoupled bending vibrations was solved exactly. This method was also used by Graça, [6], to model the dynamic response of continuous bridge girders, despite coupled bending-torsional motion was not considered.

The trains are modelled as series of moving masses acting eccentrically at constant velocity. Thus, the corresponding inertial effects of the moving loads are considered besides the gravitational force of mass.

Both models are suitable for computational implementation and automation of the design process.

2 THE GOVERNING EQUATIONS OF COUPLED THIN-WALLED BEAMS

The governing equations that describe the static and the dynamic behaviour of thin-walled beams with arbitrary cross-section were derived by applying the Hamilton's principle, yielding

$$\begin{aligned}&\rho\left(A\ddot{\xi}_z + S_z^P\ddot{\phi}\right) - \rho\left(-S_y\ddot{\xi}_x' + I_{yy}\ddot{\xi}_z'' + I_{yz}\ddot{\xi}_y'' + I_{y\omega}\ddot{\phi}''\right) + \\ &+E\left(-S_y\xi_x''' + I_{yy}\xi_z''''+ I_{yz}\xi_y''''+ I_{y\omega}\phi''''\right) = f_z\end{aligned} \tag{1}$$

$$\begin{aligned}&\rho\left(A\ddot{\xi}_y - S_y^P\ddot{\phi}\right) - \rho\left(-S_z\ddot{\xi}_x' + I_{zy}\ddot{\xi}_z'' + I_{zz}\ddot{\xi}_y'' + I_{z\omega}\ddot{\phi}''\right) + \\ &+E\left(-S_z\xi_x''' + I_{zy}\xi_z''''+ I_{zz}\xi_y''''+ I_{z\omega}\phi''''\right) = f_y\end{aligned} \tag{2}$$

$$\begin{aligned}&\rho\left(S_z^P\ddot{\xi}_z - S_y^P\ddot{\xi}_y + I_0^P\ddot{\phi}\right) - \rho\left(-S_\omega\ddot{\xi}_x' + I_{\omega y}\ddot{\xi}_z'' + I_{\omega z}\ddot{\xi}_y'' + I_{\omega\omega}\ddot{\phi}''\right) + \\ &+E\left(-S_\omega\xi_x''' + I_{\omega y}\xi_z''''+ I_{\omega z}\xi_y''''+ I_{\omega\omega}\phi''''\right) - GJ\phi'' = m_x\end{aligned} \tag{3}$$

where primes indicate differentiation with respect to the spatial coordinate x and dots represent derivatives with respect to time t. The variable E represents the modulus of elasticity,

G is the shear modulus, J is the torsion constant, A is the cross-section area, S_i and I_{ij} are respectively the first and second moments of inertia, with $\{i,j\}=\{y,z\}$, and S_ω and $I_{\omega\omega}$ correspond to the first and the second sectorial moments, respectively. The generalized displacements ξ_x, ξ_z, ξ_y and ϕ and the applied loading f_z, f_y and m_x are illustrated in Figure 1.

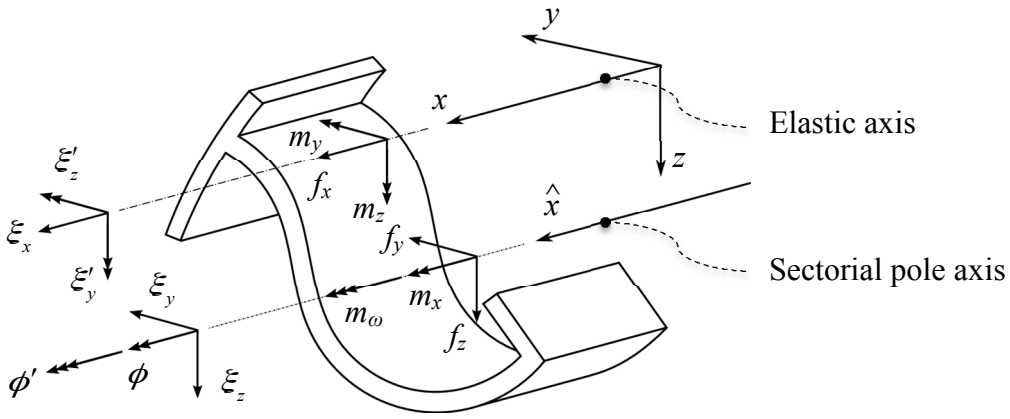

Figure 1: Element loading and generalized displacements.

For mono-symmetric cross-sections, being z the axis of symmetry, and considering the principal global coordinate system (x,y,z), the principal sectorial pole P and origin O, the dynamic equilibrium of the bridge's girder is given by

$$\rho A\ddot{\xi}_z + EI_{yy}\xi_z'''' = f_z \tag{4}$$

$$\rho\left(A\ddot{\xi}_y - S_y^P\ddot{\phi}\right) + EI_{zz}\xi_y'''' = f_y \tag{5}$$

$$\rho\left[-S_y^P\ddot{\xi}_y + \left(I_{zz}^P + I_{yy}^P\right)\ddot{\phi}\right] + EI_{\omega\omega}\phi'''' - GJ\phi'' = m_x \tag{6}$$

being the warping effect included and the rotary inertia of the cross-sections neglected.

3 FINITE ELEMENT SOLUTION

The developed beam finite element considers the six nodal degrees-of-freedom of a three-dimensional Euler-Bernoulli beam and an additional warping degree-of-freedom. This represents the out-of-plane displacements of the cross-sections when a beam is loaded in torsion. As depicted in Figure 2, the generalized displacements are referred to the centre of gravity, which motivates the presence of coupling terms in the element matrices.

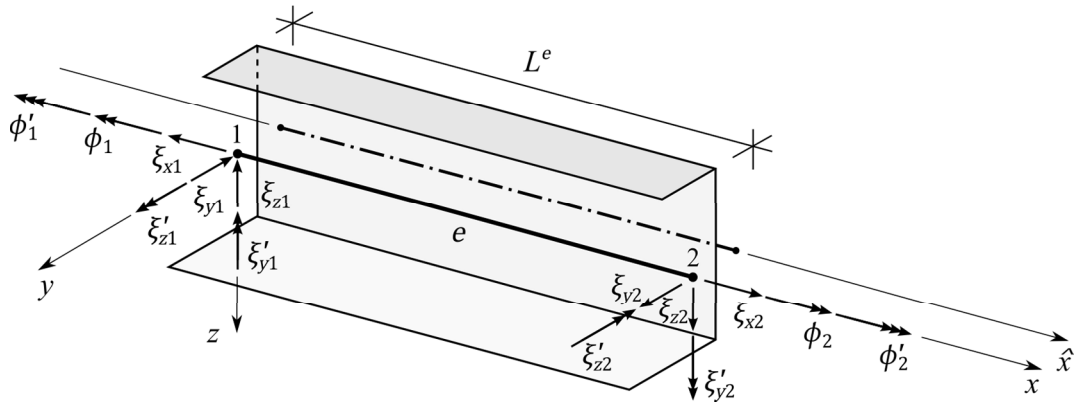

Figure 2: Beam element and the corresponding nodal degrees-of-freedom referred to the centre of gravity.

The element axial displacements ξ_x^e are approximated by Lagrange's interpolation functions, whilst Hermite's cubic interpolation functions are suitable to the bending displacements ξ_z^e and ξ_y^e and to the torsional rotations ϕ.

By applying the Galerkin's method, the governing equations are restated in the matrix form as follows:

$$\mathbf{M}^e\ddot{\boldsymbol{u}}^e + \mathbf{C}^e\dot{\boldsymbol{u}}^e + \mathbf{K}^e\boldsymbol{u}^e = \mathbf{f}^e \tag{7}$$

where $\mathbf{M}^e$ is the element mass matrix, $\mathbf{C}^e$ is the element damping matrix, $\mathbf{K}^e$ is the element stiffness matrix and $\mathbf{f}^e$ is the element external force vector. In [7], these matrices are thoroughly derived, being therein presented explicit expressions for their calculation.

The structural response to a time-dependent loading involves the solution of the differential equation (7) in time. To this end, the Newmark's β method is used, [8].

4 ANALYTICAL SOLUTION

In this section, it is proposed an analytical model to perform the dynamic analysis of continuous thin-walled beams with mono-symmetric cross-section. The natural frequencies and the corresponding mode shapes of vibration are met exactly and the modal superposition method is used to determine the structural response to moving loads. The Newmark's β method is applied to integrate of the governing equations in time.

The developed formulation considers an N-span bridge of total length L, as depicted in Figure 3, subjected to moving loads f_z, f_y and m_x of the form

$$f_z(x,t) = \sum_k^{n_{load}} \delta\left(x - x_k(t)\right) V_{zk}(t) \tag{8}$$

$$f_y(x,t) = \sum_k^{n_{load}} \delta\left(x - x_k(t)\right) V_{yk}(t) \tag{9}$$

$$m_x(x,t) = \sum_k^{n_{load}} \delta\left(x - x_k(t)\right) M_{xk}(t) \tag{10}$$

being $x_k(t)$ the position of the k-th load, $\delta(t)$ the Dirac delta function, n_{load} the number of loads, V_{ik} the k-th force parallel to the i-axis and M_{xk} the resulting torsion moment.

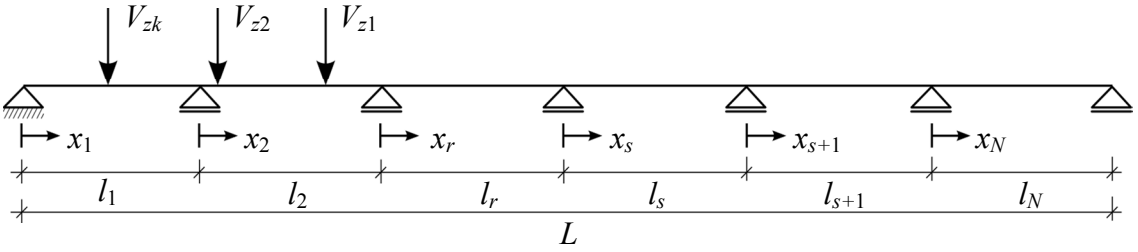

Figure 3: Model of the N-span bridge considered in the analytical formulation.

Considering that the generalized displacements are approximated by harmonic functions, the homogeneous solution of the equations (4)-(6) is given by

$$-\rho A p^2 \Xi_z(x) + EI_{yy}\Xi_z''''(x) = 0 \tag{11}$$

$$-\rho A p^2 \Xi_y(x) + \rho S_y^P p^2 \Phi(x) + EI_{zz}\Xi_y''''(x) = 0 \tag{12}$$

$$\rho S_y^P p^2 \Xi_y(x) - \rho\left(I_{zz}^P + I_{yy}^P\right) p^2 \Phi(x) + EI_{\omega\omega}\Phi''''(x) - GJ\Phi''(x) = 0 \tag{13}$$

being Ξ_z, Ξ_y and Φ the shape functions of the vertical displacement ξ_z, lateral displacement ξ_y and torsional rotation ϕ, respectively, and p is a circular frequency.

In the case of mono-symmetric cross-sections, being z the axis of symmetry, the bending vibrations in the xz-plane are decoupled. Thus, the equation (11) reduces to

$$-\lambda^4 \Xi_z(x) + \Xi_z''''(x) = 0 \tag{14}$$

where the frequency parameter λ is obtained by

$$\lambda^4 = \frac{\rho A p^2}{EI_{yy}} \tag{15}$$

The solution Ξ_z of the equation (11) is given in trigonometric and hyperbolic terms by

$$\Xi_z(x) = \mathcal{A}_1 \cosh(\lambda x) + \mathcal{A}_2 \sinh(\lambda x) + \mathcal{A}_3 \cos(\lambda x) + \mathcal{A}_4 \sin(\lambda x) \tag{16}$$

being the $\mathcal{A}_j$ constants such that the boundary conditions are satisfied. This allows expressing three of the constants $\mathcal{A}_j$ as functions of the fourth, which represents an arbitrary amplitude of the mode shape.

For the case of coupled bending-torsional vibrations in the xy-plane, the solutions Ξ_y and Φ of the equations (12)-(13) involve some mathematical treatment. By combining these two equations into one equation, eliminating either Ξ_y or Φ, [9], it is possible to obtain the following ordinary differential equation:

$$\left[dD^8 - D^6 - \left(a + bd\right) D^4 + bD^2 + abc \right] \chi(x) = 0 \tag{17}$$

being χ either Ξ_y or Φ, D is a differential operator in order to x, and the remaining parameters given by

$$a = \left(I_{zz}^P + I_{yy}^P \right) \frac{\rho p^2}{GJ} \qquad b = \frac{\rho A p^2}{EI_{zz}} \qquad c = 1 - \frac{S_y^{P2}}{A\left(I_{zz}^P + I_{yy}^P \right)} \qquad d = \frac{EI_{\omega\omega}}{GJ} \tag{18}$$

Considering an exponential solution for the differential equation (17) and performing a change of variables, the following quartic polynomial is obtained:

$$d\eta^4 - \eta^3 - \left(a + bd\right)\eta^2 + b\eta + abc = 0 \tag{19}$$

Since, for a physical problem, the coefficients a, b, c and d are always positive reals, being c less than one, it is possible to show, [10] that all eight roots of the polynomial (19) are

$$\alpha, \quad -\alpha, \quad \beta, \quad -\beta, \quad \square\gamma, \quad -\square\gamma, \quad \square\delta \text{ and } -\square\delta \tag{20}$$

where

$$\alpha = \sqrt{\eta_1}, \quad \beta = \sqrt{\eta_2}, \quad \gamma = \sqrt{\eta_3}, \quad \delta = \sqrt{\eta_4} \quad \text{and} \quad i = \sqrt{-1} \tag{21}$$

being η_1, η_2, $-\eta_3$ and $-\eta_4$ the four real roots of equation (19).

Thus, obtaining the solution χ of the equation (17), the lateral bending displacement Ξ_y and the torsional rotation Φ are defined as follows:

$$\Xi_y(x) = \mathcal{B}_1\cosh(\alpha x) + \mathcal{B}_2\sinh(\alpha x) + \mathcal{B}_3\cosh(\beta x) + \mathcal{B}_4\sinh(\beta x) + \\ + \mathcal{B}_5\cos(\gamma x) + \mathcal{B}_6\sin(\gamma x) + \mathcal{B}_7\cos(\delta x) + \mathcal{B}_8\sin(\delta x) \tag{22}$$

$$\Phi(x) = \mathcal{C}_1\cosh(\alpha x) + \mathcal{C}_2\sinh(\alpha x) + \mathcal{C}_3\cosh(\beta x) + \mathcal{C}_4\sinh(\beta x) + \\ + \mathcal{C}_5\cos(\gamma x) + \mathcal{C}_6\sin(\gamma x) + \mathcal{C}_7\cos(\delta x) + \mathcal{C}_8\sin(\delta x) \tag{23}$$

The relations between the two sets of constant $\mathcal{B}_j$ and $\mathcal{C}_j$ are given by

$$\mathcal{C}_1 = \kappa_\alpha\mathcal{B}_1, \quad \mathcal{C}_2 = \kappa_\alpha\mathcal{B}_2, \quad \mathcal{C}_3 = \kappa_\beta\mathcal{B}_3, \quad \mathcal{C}_4 = \kappa_\beta\mathcal{B}_4, \\ \mathcal{C}_5 = \kappa_\gamma\mathcal{B}_5, \quad \mathcal{C}_6 = \kappa_\gamma\mathcal{B}_6, \quad \mathcal{C}_7 = \kappa_\delta\mathcal{B}_7, \quad \mathcal{C}_8 = \kappa_\delta\mathcal{B}_8, \tag{24}$$

where the coefficients κ_α, κ_β, κ_γ and κ_δ are defined as follows:

$$\kappa_\alpha = \frac{\rho Ap^2 - EI_{zz}\alpha^4}{\rho S_y^P p^2}, \ \kappa_\beta = \frac{\rho Ap^2 - EI_{zz}\beta^4}{\rho S_y^P p^2}, \ \kappa_\gamma = \frac{\rho Ap^2 - EI_{zz}\gamma^4}{\rho S_y^P p^2}, \ \kappa_\delta = \frac{\rho Ap^2 - EI_{zz}\delta^4}{\rho S_y^P p^2} \tag{25}$$

In order to obtain the *n*-th frequency of vibration of the considered structure, the equations (16), (22) and (23) are applied to each span *s* along with the corresponding boundary conditions, as illustrated in Figure 4. The frequency of vibration is given by the equations that define the static boundary conditions at the last support of the span *N*. This assembly procedure was used by Chan and Ashebo, [5], being extended in the present work to coupled vibrations.

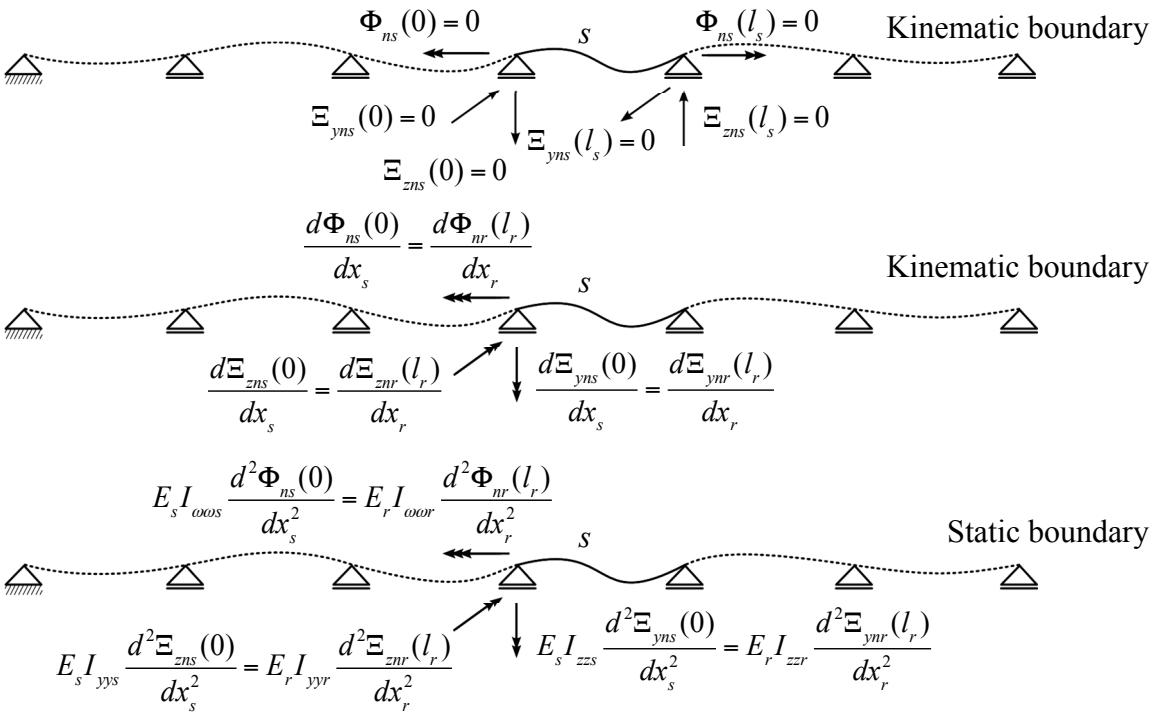

Figure 4: Boundary conditions at the supports of a generic span *s*.

The constants $\mathcal{A}_{jns}$ and $\mathcal{B}_{jns}$, resulting from the application of shape functions to the *s*-th span, are calculated by imposing the following static and kinematic boundary conditions at the corresponding supports:

$$\Xi_{zns}(0) = 0, \quad \Xi_{zns}(l_s) = 0, \quad \Xi_{yns}(0) = 0, \quad \Xi_{yns}(l_s) = 0, \quad \Phi_{ns}(0) = 0, \quad \Phi_{ns}(l_s) = 0 \tag{26}$$

$$\frac{d\Xi_{zns}(0)}{dx_s} = \frac{d\Xi_{znr}(l_r)}{dx_r}, \quad \frac{d\Xi_{yns}(0)}{dx_s} = \frac{d\Xi_{ynr}(l_r)}{dx_r}, \quad \frac{d\Phi_{ns}(0)}{dx_s} = \frac{d\Phi_{nr}(l_r)}{dx_r} \tag{27}$$

$$E_s I_{yys} \frac{d^2\Xi_{zns}(0)}{dx_s^2} = E_r I_{yyr} \frac{d^2\Xi_{znr}(l_r)}{dx_r^2}, \quad E_s I_{zzs} \frac{d^2\Xi_{yns}(0)}{dx_s^2} = E_r I_{zzr} \frac{d^2\Xi_{ynr}(l_r)}{dx_r^2}$$
$$\text{and} \quad E_s I_{\omega\omega s} \frac{d^2\Phi_{ns}(0)}{dx_s^2} = E_r I_{\omega\omega r} \frac{d^2\Phi_{nr}(l_r)}{dx_r^2} \tag{28}$$

The case of decoupled vertical bending vibrations is firstly considered. By substituting the corresponding boundary conditions (26)-(28) in the equation (16), and considering that one of the four $\mathcal{A}_{jn1}$ constants, relative to the first span, represent an arbitrary amplitude of the shape function Ξ_{zn1}, yields

$$\mathcal{A}_{1n1} = 0, \quad \mathcal{A}_{2n1} = 1, \quad \mathcal{A}_{3n1} = 0, \quad \mathcal{A}_{4n1} = -\frac{\sinh(\lambda_{n1} l_1)}{\sin(\lambda_{n1} l_1)} \tag{29}$$

and for the *s*-th inner span

$$\mathcal{A}_{1ns} = \frac{1}{2} \frac{E_r I_{yyr}}{E_s I_{yys}} \frac{\lambda_{nr}^2}{\lambda_{ns}^2} \left[\mathcal{A}_{1nr} \cosh(\lambda_{nr} l_r) + \mathcal{A}_{2nr} \sinh(\lambda_{nr} l_r) - \mathcal{A}_{3nr} \cos(\lambda_{nr} l_r) - \mathcal{A}_{4nr} \sin(\lambda_{nr} l_r) \right] \tag{30}$$

$$\mathcal{A}_{2ns} = \frac{\lambda_{nr}}{\lambda_{ns}} \left[\mathcal{A}_{1nr} \sinh(\lambda_{nr} l_r) + \mathcal{A}_{2nr} \cosh(\lambda_{nr} l_r) - \mathcal{A}_{3nr} \sin(\lambda_{nr} l_r) - \mathcal{A}_{4nr} \cos(\lambda_{nr} l_r) \right] \times$$
$$\times \frac{\sin(\lambda_{ns} l_s)}{\sin(\lambda_{ns} l_s) - \sinh(\lambda_{ns} l_s)} - \mathcal{A}_{1ns} \frac{\cos(\lambda_{ns} l_s) - \cosh(\lambda_{ns} l_s)}{\sin(\lambda_{ns} l_s) - \sinh(\lambda_{ns} l_s)} \tag{31}$$

$$\mathcal{A}_{3ns} = -\mathcal{A}_{1ns} \tag{32}$$

$$\mathcal{A}_{4ns} = \frac{\lambda_{nr}}{\lambda_{ns}} \left[\mathcal{A}_{1nr} \sinh(\lambda_{nr} l_r) + \mathcal{A}_{2nr} \cosh(\lambda_{nr} l_r) - \mathcal{A}_{3nr} \sin(\lambda_{nr} l_r) + \mathcal{A}_{4nr} \cos(\lambda_{nr} l_r) \right] - \mathcal{A}_{2ns} \tag{33}$$

Imposing the boundary condition on the bending moment at the last support of the span *N*, the following equation is obtained:

$$\mathcal{A}_{1nN} \cosh(\lambda_{nN} l_N) + \mathcal{A}_{2nN} \sinh(\lambda_{nN} l_N) - \mathcal{A}_{3nN} \cos(\lambda_{nN} l_N) - \mathcal{A}_{4nN} \sin(\lambda_{nN} l_N) = 0 \tag{34}$$

which roots give the natural frequencies for the decoupled vertical bending motion. In the work of Chan and Ashebo, [5], the equation (34) is not presented, being the procedure of finding the natural frequencies unclear.

The frequencies of the coupled lateral bending-torsional vibrations are determined through a similar procedure. By substituting the remaining boundary conditions (26)-(28) in the equations (22)-(23), the eight $\mathcal{B}_{jn1}$ constants of the first span are given by

$$\mathcal{B}_{1n1} = 0, \quad \mathcal{B}_{3n1} = 0, \quad \mathcal{B}_{5n1} = 0, \quad \mathcal{B}_{7n1} = 0 \tag{35}$$

$$\mathcal{B}_{6n1} = \frac{\mathcal{B}_{2n1} \sinh(\alpha_{n1} l_1)(\kappa_{\delta 1} - \kappa_{\alpha 1}) + \mathcal{B}_{4n1} \sinh(\beta_{n1} l_1)(\kappa_{\delta 1} - \kappa_{\beta 1})}{\sin(\gamma_{n1} l_1)(\kappa_{\gamma 1} - \kappa_{\delta 1})} \tag{36}$$

$$\mathcal{B}_{8n1} = \frac{\mathcal{B}_{2n1}\sinh(\alpha_{n1}l_1)(\kappa_{\alpha1}-\kappa_{\gamma1}) + \mathcal{B}_{4n1}\sinh(\beta_{n1}l_1)(\kappa_{\beta1}-\kappa_{\gamma1})}{\sin(\delta_{n1}l_1)(\kappa_{\gamma1}-\kappa_{\delta1})} \tag{37}$$

For the generic inner span s the expressions of the eight constants $\mathcal{B}_{jns}$ may be easily obtained using symbolic algebra software. Once computed the explicit expressions for the constants $\mathcal{B}_{jns}$, it is straightforward to apply the presented analytical procedure to girders with any number of spans.

The n-th frequency of vibration is obtained by imposing the boundary conditions on the bending moment and the bimoment at the last support of the span N. These conditions can be written as functions of $\mathcal{B}_{2n1}$ and $\mathcal{B}_{4n1}$, yielding

$$\begin{bmatrix} S_{22} & S_{24} \\ S_{42} & S_{44} \end{bmatrix} \begin{Bmatrix} \mathcal{B}_{2n1} \\ \mathcal{B}_{4n1} \end{Bmatrix} = \mathbf{0} \tag{38}$$

where the matrix components S_{kl} are determined by making $\mathcal{B}_{kn1}$ and $\mathcal{B}_{ln1}$ equal to zero and one, respectively, when the first span is evaluated, i.e., in equations (35)-(37). By giving $\mathcal{B}_{2n1}$ a unit value, the $\mathcal{B}_{jn1}$ constants are rewritten as follows:

$$\mathcal{B}_{1n1} = 0, \quad \mathcal{B}_{3n1} = 0, \quad \mathcal{B}_{5n1} = 0, \quad \mathcal{B}_{7n1} = 0, \quad \mathcal{B}_{2n1} = 1, \quad \mathcal{B}_{4n1} = -\frac{S_{22}}{S_{24}} \tag{39}$$

$$\mathcal{B}_{6n1} = \frac{S_{24}\sinh(\alpha_{n1}l_1)(\kappa_{\delta1}-\kappa_{\alpha1}) + S_{22}\sinh(\beta_{n1}l_1)(\kappa_{\beta1}-\kappa_{\delta1})}{S_{24}\sin(\gamma_{n1}l_1)(\kappa_{\gamma1}-\kappa_{\delta1})} \tag{40}$$

$$\mathcal{B}_{8n1} = \frac{S_{24}\sinh(\alpha_{n1}l_1)(\kappa_{\alpha1}-\kappa_{\gamma1}) + S_{22}\sinh(\beta_{n1}l_1)(\kappa_{\gamma1}-\kappa_{\beta1})}{S_{24}\sin(\delta_{n1}l_1)(\kappa_{\gamma1}-\kappa_{\beta1})} \tag{41}$$

Finally, the n-th frequency of vibration for the coupled bending-torsional motion is calculated be seeking for the roots of the equation

$$\det\left(\begin{bmatrix} S_{22} & S_{24} \\ S_{42} & S_{44} \end{bmatrix}\right) = 0 \tag{42}$$

Once the frequencies of vibration have been calculated, the m- and the n-th mode shape, in which the continuous beam is said to respond when vibrates with a frequency p_m or p_n, is established by the explicit expressions

$$\Xi_{zm}(x) = \sum_{s=1}^{N}\left[\mathrm{H}(x-\sum_{r=1}^{s-1}l_r) - \mathrm{H}(x-\sum_{r=1}^{s}l_r)\right]\Xi_{zms}(x_s) \tag{43}$$

$$\Xi_{yn}(x) = \sum_{s=1}^{N}\left[\mathrm{H}(x-\sum_{r=1}^{s-1}l_r) - \mathrm{H}(x-\sum_{r=1}^{s}l_r)\right]\Xi_{yns}(x_s) \tag{44}$$

$$\Phi_{n}(x) = \sum_{s=1}^{N}\left[\mathrm{H}(x-\sum_{r=1}^{s-1}l_r) - \mathrm{H}(x-\sum_{r=1}^{s}l_r)\right]\Phi_{ns}(x_s) \tag{45}$$

being H the Heaviside step function.

To quantify the damping properties, it is established a proportional relation to the modal mass properties. Considering the modal superposition method, the beam's generalized displacements ξ_z, ξ_y and ϕ are redefined as

$$\xi_z(x,t) = \sum_k^{\infty} \Xi_{zk}(x)\, \Psi_k(t) \tag{46}$$

$$\xi_y(x,t) = \sum_l^{\infty} \Xi_{yl}(x)\, \Upsilon_l(t) \tag{47}$$

$$\phi(x,t) = \sum_l^{\infty} \Phi_l(x)\, \Upsilon_l(t) \tag{48}$$

where Ψ_k and ®$_l$ are the time-varying amplitudes of the k-th and the l-th vibration modes.

By applying the Betti's law, the orthogonality conditions of the vibration mode shapes m and n with respect to mass yield

$$\int_0^L \Xi_{zm}(x)\, \Xi_{zn}(x)\, dx = 0 \tag{49}$$

$$\int_0^L \left[\rho A\, \Xi_{ym}(x)\, \Xi_{yn}(x) + \rho \left(I_{zz}^P + I_{yy}^P \right) \Phi_m(x)\, \Phi_n(x) \right] dx = 0 \tag{50}$$

The decoupling of the governing equations (4)-(6) is accomplished by considering the modal coordinate expressions (46)-(47), leading to

$$M_{zm} \ddot{\Psi}_m(t) + C_{zm} \dot{\Psi}_m(t) + p_m^2 M_{zm} \Psi_m(t) = P_{zm}(t) \tag{51}$$

$$M_{y\phi n} \ddot{\Upsilon}_n(t) + C_{y\phi n} \dot{\Upsilon}_n(t) + p_n^2 M_{y\phi n} \Upsilon_n(t) = P_{y\phi n}(t) \tag{52}$$

where

$$M_{zm} = \rho A \int_0^L \Xi_{zm}^2(x)\, dx, \quad C_{zm} = 2\xi_{zm} p_m M_{zm}, \quad P_{zm} = \int_0^L \Xi_{zm}(x) f_z(x,t)\, dx \tag{53}$$

$$\begin{aligned} &M_{y\phi n} = \int_0^L \left[\rho A\, \Xi_{yn}^2(x) + \rho \left(I_{zz}^P + I_{yy}^P \right) \Phi_n^2(x) \right] dx, \quad C_{y\phi n} = 2\xi_{y\phi n} p_n M_{y\phi n} \\ &\text{and} \quad P_{y\phi n} = \int_0^L \left[\Xi_{yn}(x) f_y(x,t) + \Phi_n(x) m_x(x,t) \right] dx \end{aligned} \tag{54}$$

being ξ_{zm} and $\xi_{y\phi n}$ the modal viscous damping ratios of each vibration mode.

The dynamic response of the structure under the action of moving loads is obtained by applying the Newmark's β method to the equations (51)-(52).

5 DYNAMIC RESPONSE OF CONTINUOUS BEAMS UNDER MOVING LOADS

In the sequel, the proposed numerical and the analytical beam models are applied in order to perform the dynamic analysis of a multi-span bridge eccentrically traversed by moving vehicles. The longitudinal model is shown in Figure 5 and the prescribed boundary conditions at the supports are listed in Table 2. The dynamic responses are obtained by taking into account the high-speed universal trains HSLM-A10 proposed by the EN 1991-2, [11], travelling at 80 and 120 ms^{-1}. The mass effect of the moving loads is also considered.

An open double-T cross section is considered, being the material and the geometrical properties presented in Table 1.

E (kN/m^2)	G (kN/m^2)	ρ (ton/m^3)	A (m^2)	J (m^4)	I_{yy} (m^4)	I_{zz} (m^4)	$I_{z\omega}$ (m^5)
33000	13750	2.55	9.51	1.22	9.16	122.37	175.74

Table 1: Material and geometrical properties of the cross-section considered in the examples.

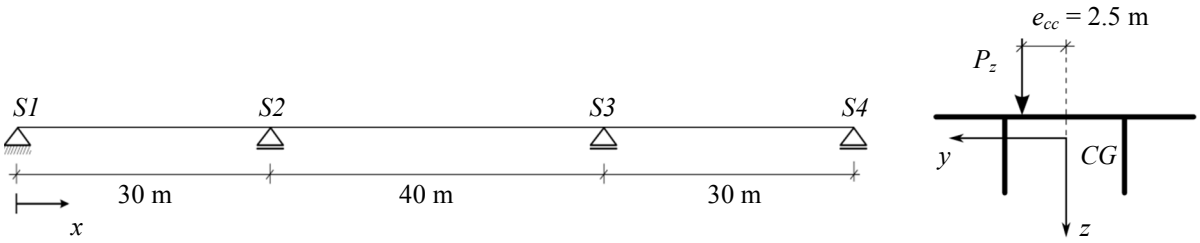

Figure 5: Longitudinal model of the considered three-span girder.

Support	Nodal Coordinate	Kinematic Boundary Conditions	Static Boundary Conditions
S1	$x = 0$ m	$\xi_z(x) = \xi_y(x) = \phi(x) = 0$	$\xi_z''(x) = \xi_y''(x) = \phi''(x) = 0$
S2	$x = 30$ m	$\xi_z(x) = \xi_y(x) = \phi(x) = 0$ $\xi_z'(x^-) = \xi_z'(x^+)$	$\xi_z''(x^-) = \xi_z''(x^+)$ $\xi_y''(x^-) = \xi_y''(x^+)$
S3	$x = 70$ m	$\xi_y'(x^-) = \xi_y'(x^+)$ $\phi'(x^-) = \phi'(x^+)$	$\phi''(x^-) = \phi''(x^+)$
S4	$x = 100$ m	$\xi_z(x) = \xi_y(x) = \phi(x) = 0$	$\xi_z''(x) = \xi_y''(x) = \phi''(x) = 0$

Table 2: Prescribed boundary conditions at the supports of the three-span girder.

The natural frequencies calculated by the two beam models are compared in Table 3 with the values given by the shell finite element model.

The dynamic influence lines of the vertical displacements and accelerations at the track's mid-point of the central span are presented in Figure 6 and Figure 7.

Frequencies of Vibration in the plane *xz* (Hz)			
Frequency Number	Model of Analysis		
	Numerical	Analytical	Shell FEM
1	4.58	4.59	4.43
2	7.48	7.52	7.05
3	8.97	9.02	8.19
4	17.07	17.29	15.05
5	25.84	26.40	22.20
6	28.18	28.78	23.31

Frequencies of Vibration in the plane *xy* (Hz)			
Frequency Number	Model of Analysis		
	Numerical	Analytical	Shell FEM
1	4.87	4.89	4.76
2	7.41	7.45	7.10
3	8.53	8.57	7.91
4	15.78	15.93	14.11
5	17.17	18.11	12.74
6	23.55	23.94	20.46

Table 3: Natural frequencies of vibration of the considered girder.

In the next, the mass effect of the moving vehicles is taken into account in the dynamic response of the three-span girder. Therefore, the considered loading is written as follows:

$$f_z(x,t) = \sum_k^{n_{load}} \delta\big(x - x_k(t)\big)\left[V_{zk}(t) - m_k \frac{d^2 v_k}{dt^2}\right] \quad \text{and} \quad m_x(x,t) = f_z(x,t)\, e_{cc} \tag{55}$$

being $x_k(t)$ the position and m_k the mass of the k-th load, v_k is the vertical displacement of the moving mass m_k, δ the Dirac delta function, n_{load} the number of loads and e_{cc} is the eccentricity of the track's position.

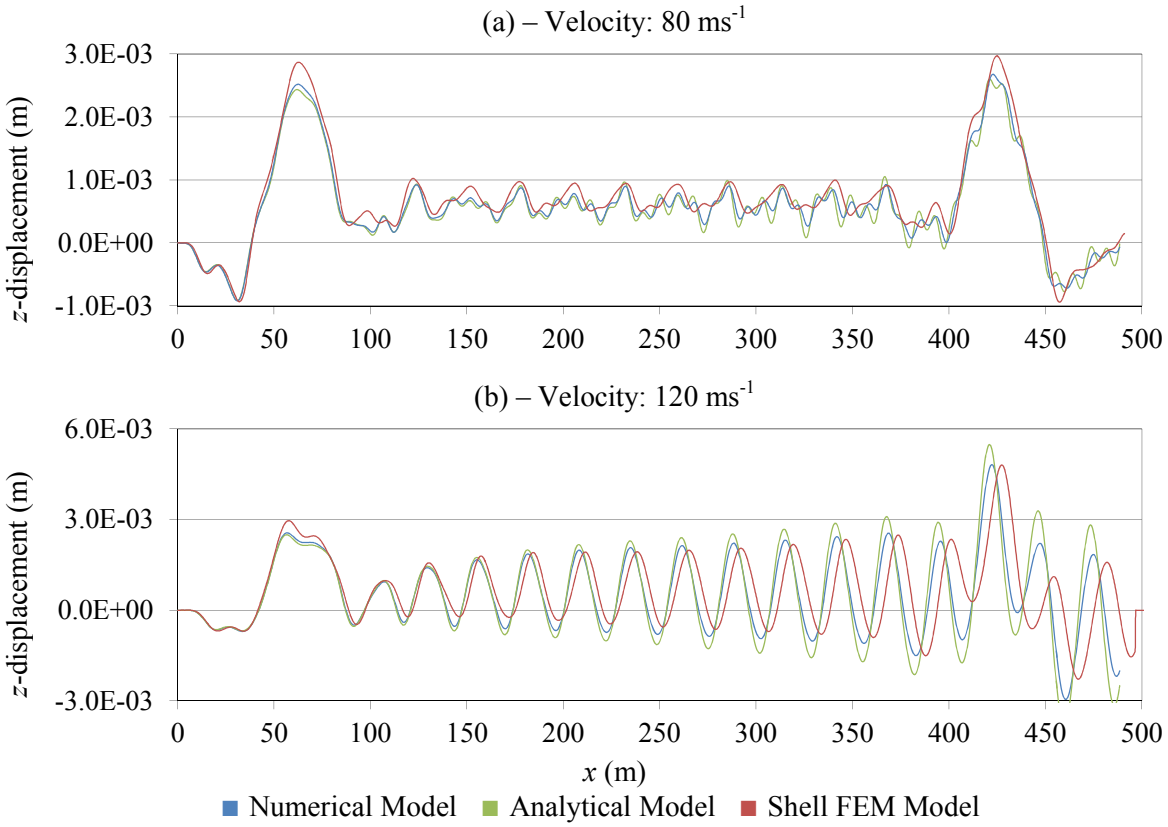

Figure 6: Dynamic influence lines of the z-displacement at the track's mid-point of the central span.

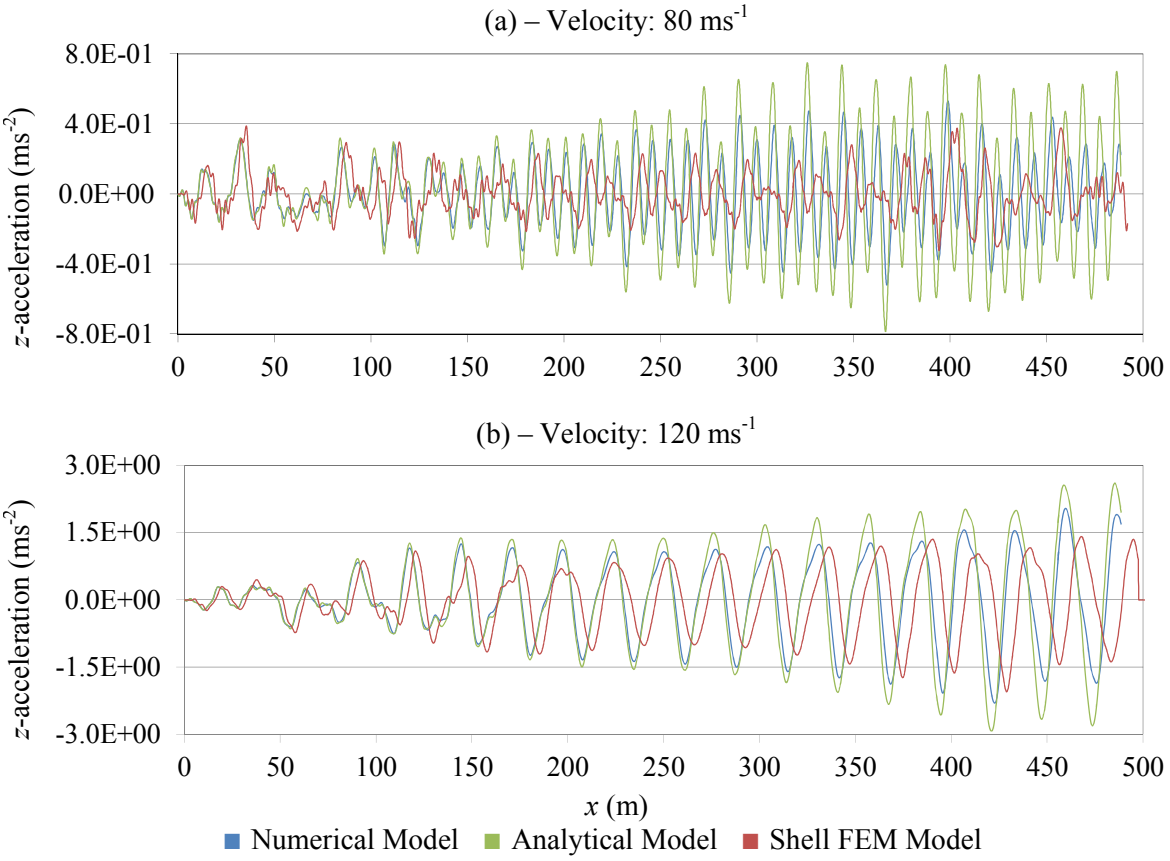

Figure 7: Dynamic influence lines of the z-acceleration at the track's mid-point of the central span.

Since the load is acting on a moving coordinate, v_k and its derivatives with respect to time t are given as follows, [12]:

$$v_k(t) = \xi_z(ct,t), \quad \frac{dv_k}{dt} = \frac{\partial \xi_z}{\partial t} + c\frac{\partial \xi_z}{\partial x}, \quad \frac{d^2v_k}{dt^2} = \frac{\partial^2 \xi_z}{\partial t^2} + 2c\frac{\partial \xi_z}{\partial t}\frac{\partial \xi_z}{\partial x} + c^2\frac{\partial^2 \xi_z}{\partial x^2} \tag{56}$$

where c represents the velocity of the moving masses. Notice that it is assumed that the masses do not separate from the beam during their travel and vertical vibration.

In Figure 8 the dynamic response considering the mass of the vehicles is represented. The influence of constrained warping is also evaluated by using the numerical model. It is observed that both the displacements and accelerations in the z direction are lower than when the warping effect is considered.

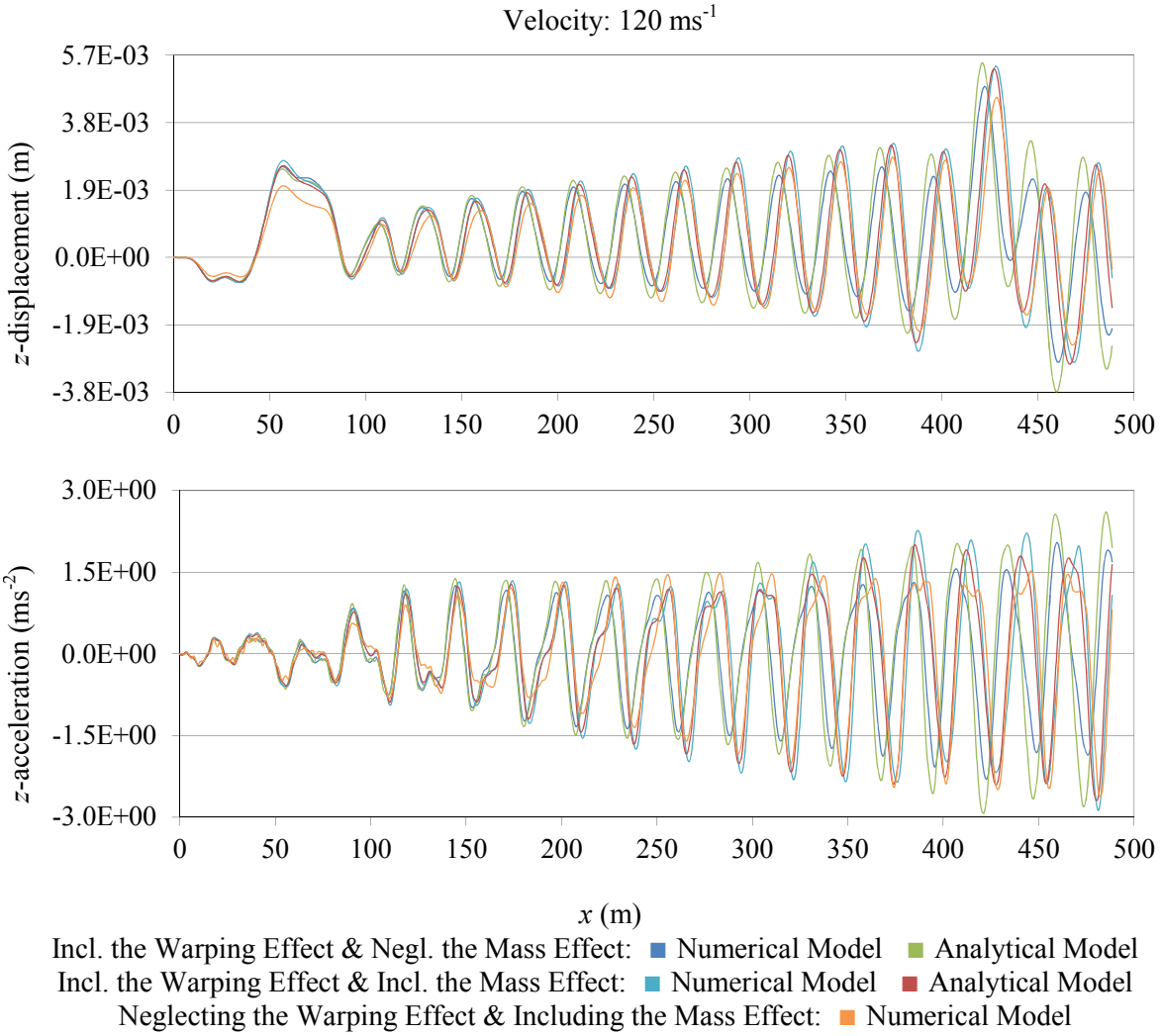

Figure 8: Influence of the mass effect on the influence lines of the z-displacement at the track's mid-point of the central span.

6 CONCLUSION

The main objective of the present work was to provide two beam models capable of performing dynamic analyses of railway bridges, being considered the warping displacements and the mass effects of the moving loads.

In the previous sections, a *numerical* and an *analytical* beam models were developed and applied to the analysis of an open cross-section girder. The torsional response was shown to be significantly influenced by the warping deformations.

The developed beam models gave good results, being in good agreement with the shell finite element model implemented in commercial software. Thus, the developed models perform efficient dynamic analyses that consider the warping effect, which may be very useful at early design stages.

The presented models could serve as a starting point for further in-depth study of the subject and may be considered as a first step tending to more complete formulations accounting for other aspects that have not been considered.

REFERENCES

[1] D. Lisi, *A Beam Finite Element Model Including Warping – Application to the Dynamic and Static Analysis of Bridge Decks*, IST, Técnico Lisboa, 2011.

[2] D.S. Sophianopoulos and G.T. Michaltsos, Combined torsional-lateral vibrations of beams under vehicular loading – I: formulation and solution techniques, *Automatic Control & Robotics*, 2, 877-886, 1999.

[3] L.T. Stayridis and G.T. Michaltsos, Eigenfrequency analysis of thin-walled girders curved in plan, *Journal of Sound and Vibration*, 227, 383-396, 1999.

[4] G.T. Michaltsos, E. Sarantithou and D.S. Sophianopoulos, Flexural-torsional vibration of simply supported open cross-section steel beams under moving loads, *Journal of Sound and Vibration*, 280, 479-494, 2005.

[5] T.H.T. Chan and D.B. Ashebo, Theoretical study of moving force identification on continuous bridges, *Journal of Sound and Vibration*, 295, 870-883, 2006.

[6] A. Graça, *Modelação da Resposta em Pontes Devido à Passagem de Comboios de Alta Velocidade – formulação e implementação computacional de um modelo para simulação do efeito da passagem de comboios de alta velocidade em pontes*, Master Dissertation, IST, Técnico Lisboa, 2011.

[7] J. Serra, *Dynamic Analysis of Bridge Girders Subjected to Moving Loads – Numerical and Analytical Beam Models Considering Warping Effects*, IST, Técnico Lisboa, 2014.

[8] W. Wunderlich and W.D. Pilkey, *Mechanics of Structures – Variational and Computational Methods*, Second Edition, CRC Press, 2003.

[9] J.R. Banerjee, S. Guo and W.P. Howson, Exact dynamic stiffness matrix of a bending-torsion coupled beam including warping, *Computers & Structures*, 59(4), 613-621, 1996.

[10] R.E.D. Bishop, S.M. Cannon and S. Miao, On coupled bending and torsional vibration of uniform beams, *Journal of Sound and Vibration*, 131(3), 457-464, 1989.

[11] EN 1991-2: Actions on structures – Part 2: Traffic loads on bridges, CEN – European Commitee for Standardization.

[12] H. Ouyang, Moving-load dynamic problems: A tutorial (with brief overview), *Mechanical Systems and Signal Processing*, 25, 2039-2060, 2011.